JACS
JOURNAL OF THE AMERICAN CHEMICAL SOCIETY
Article
pubs.acs.org/JACS

Reverse Micelles As a Platform for Dynamic Nuclear Polarization in Solution NMR of Proteins

Kathleen G. Valentine,[†] Guinevere Mathies,[‡] Sabrina Bédard,[†] Nathaniel V. Nucci,[†] Igor Dodevski,[†] Matthew A. Stetz,[†] Thach V. Can,[‡] Robert G. Griffin,[‡] and A. Joshua Wand*[,†]

[†]Johnson Research Foundation and Department of Biochemistry and Biophysics, University of Pennsylvania, Philadelphia, Pennsylvania 19104-6059

[‡]Francis Bitter Magnet Laboratory and Department of Chemistry, Massachusetts Institute of Technology, Cambridge, Massachusetts 02139

ABSTRACT: Despite tremendous advances in recent years, solution NMR remains fundamentally restricted due to its inherent insensitivity. Dynamic nuclear polarization (DNP) potentially offers significant improvements in this respect. The basic DNP strategy is to irradiate the EPR transitions of a stable radical and transfer this nonequilibrium polarization to the hydrogen spins of water, which will in turn transfer polarization to the hydrogens of the macromolecule. Unfortunately, these EPR transitions lie in the microwave range of the electromagnetic spectrum where bulk water absorbs strongly, often resulting in catastrophic heating. Furthermore, the residence times of water on the surface of the protein in bulk solution are generally too short for efficient transfer of polarization. Here we take advantage of the properties of solutions of encapsulated proteins dissolved in low viscosity solvents to implement DNP in liquids. Such samples are largely transparent to the microwave frequencies required and thereby avoid significant heating. Nitroxide radicals are introduced into the reverse micelle system in three ways: attached to the protein, embedded in the reverse micelle shell, and free in the aqueous core. Significant enhancements of the water resonance ranging up to ∼−93 at 0.35 T were observed. We also find that the hydration properties of encapsulated proteins allow for efficient polarization transfer from water to the protein. These and other observations suggest that merging reverse micelle encapsulation technology with DNP offers a route to a significant increase in the sensitivity of solution NMR spectroscopy of proteins and other biomolecules.

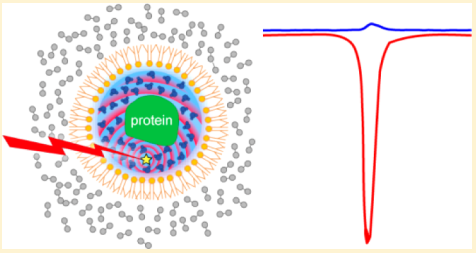

INTRODUCTION

The structural and dynamic aspects of proteins have been at center stage of our understanding of the chemical basis of their function for several decades. Nuclear magnetic resonance (NMR) in solution has contributed significantly to this view and the information inherent in NMR phenomena offers much more. Yet, despite tremendous advances in technology, experimental design and analytical strategies, solution NMR spectroscopy of macromolecules remains fundamentally restricted due to its low sensitivity. Though state-of-the-art multinuclear multidimensional NMR spectra can be routinely recorded from samples with ∼0.5 mM concentrations, many systems and problems of interest remain inaccessible due to limited solubility and/or limited availability. This is particularly true for biopolymers such as proteins and nucleic acids. Thus, a further extension of the sensitivity of the NMR method into the low μM concentration regime is highly desirable.

One approach to increasing the sensitivity of the NMR experiment is to couple the nuclear spins to a reservoir with much higher polarization, such as unpaired electrons ($\gamma_e/\gamma_H \approx -660$). In dynamic nuclear polarization (DNP) the large electron spin polarization is transferred to nuclear spins by irradiation at or near the electronic resonance. Originally proposed by Overhauser in the context of metals,[1] DNP was subsequently experimentally demonstrated in liquids.[2] Elementary models suggested that DNP in aqueous solutions would be inefficient at high magnetic fields and for this reason it was not seriously considered as a method of improving the sensitivity in high-field NMR spectroscopy.[3,4] However, in the last two decades high field DNP in both liquids and solids has enjoyed a considerable renaissance.[5] In magic angle spinning (MAS) experiments the mechanisms that mediate DNP are the solid and the cross effects and with sufficient microwave field strengths both lead to signal enhancements ε>100 at high fields up to 700 MHz for ^{1}H.[6−9] In addition, it was recently shown that it is possible to achieve significant enhancements of protons in water at magnetic fields up to 9.2 T via the Overhauser effect (OE).[10−14]

Despite these successes, application of DNP to enhance the sensitivity of solution NMR faces three significant challenges. First, water absorbs strongly in the microwave region, and can lead to significant and often catastrophic sample heating. Second, the skin depth of high frequency microwaves in water limits the penetration of the radiation into the sample. Third, transfer of polarization from the solvent to large molecules

Received: October 20, 2013
Published: January 24, 2014

   dx.doi.org/10.1021/ja4107176 | J. Am. Chem. Soc. 2014, 136, 2800−2807

(e.g., proteins) in solution has up to now not been accomplished. In this paper we propose an approach that deals with the first two challenges and has great potential in overcoming the third.

Previously, we introduced the idea of encapsulating proteins inside the protective aqueous core of a reverse micelle, which can be prepared in an ultralow viscosity fluid, thereby improving the quality of their NMR spectra.[15] The original goal was to make the entire reverse micelle particle containing the protein tumble with a correlation time that is shorter than in the relatively more viscous water. As we show below, the unique features of this type of sample largely avoids the dielectric loss (heating) and penetration issues arising from irradiation with microwave frequencies.[16−19] In addition, the slower motion of water relative to bulk solution overcomes a previously unanticipated limitation -- namely the short residence time(s) of water on the surface of protein molecules, which results in inefficient dipolar contact and poor polarization transfer to the protein. In contrast to bulk solution, the residence time of water on the surface of an encapsulated protein is significantly longer and results in excellent polarization transfer.[20,21] The reverse micelle system also offers great flexibility for introducing the polarizing agent and potentially permits the tuning of the water dynamics to optimize the DNP enhancements.

EXPERIMENTAL SECTION

Protein Expression and Spin Labeling. The C55A mutant of flavodoxin from PCC7119 was expressed during growth on minimal media containing $^{15}NH_4Cl$ as described previously.[22] This protein was used for studies where the nitroxide spin label was either free in the aqueous core of the reverse micelle or attached to a lipid embedded in the reverse micelle surfactant shell. The ^{15}N flavodoxin (C55A) with the flavin mononucleotide bound was concentrated to 6.5 mM in 10 mM Tris buffer and 100 mM NaCl at pH 8.0 for reverse micelle sample injection. To covalently attach a nitroxide spin label to the protein, a surface accessible cysteine mutant of flavodoxin (C55A, S72C) was generated by site directed mutagenesis and confirmed by DNA sequencing. Uniformly ^{15}N-labeled flavodoxin (C55A, S72C) was expressed and purified as described above except that 1 mM dithiothreitol (DTT) was present throughout the purification to prevent dimerization. Flavodoxin (C55A, S72C) was covalently labeled with ^{15}N-(1-oxyl-2,2,5,5-tetramethyl-D3-pyrroline-3-methyl)-methanethiosulfonate (MTSL) (Toronto Research Chemicals) using published protocols.[23,24] A 10-fold excess of MTSL in acetonitrile was added to a 1 mM solution of ^{15}N flavodoxin (C55A, S72C) in 10 mM Tris buffer and 100 mM NaCl at pH 8.0. No DTT was used at this point. The reaction was allowed to proceed for 16 h at room temperature under argon. The excess reagent was removed by repetitive ultrafiltration.

Reverse Micelle Sample Preparation. Solutions of reverse micelles were made with a surfactant mixture containing a 65:35 molar ratio of 1-decanoyl-rac-glycerol (10MAG) (Sigma-Aldrich, Co., LLC) and lauryl-dimethylamine-*N*-oxide (LDAO) (Affymetrix, Inc.), at 100 mM concentration, 5 mM d-11-hexanol dissolved in d-14 hexane with a molar ratio of water to total surfactant molecules (W_o or water loading) of 20.[25] LDAO and 10MAG are combined in the prescribed ratio as dry powders, dissolved in hexane, bath sonicated to promote dissolution and lyophilized in glass vials. Surfactants were pre-equilibrated to the desired pH as required.[26] Lyophilized dry mixtures of surfactants were dissolved in 0.5 mL deuterated hexane and made 5 mM in deuterated hexanol (0.3 μL). An aqueous aliquot equivalent to a water loading of 20 (18.2 μL) was injected and then vortexed, resulting in a clear solution. This procedure was followed to prepare reverse micelles containing flavodoxin-MTSL adducts or flavodoxin with TEMPOL dissolved in the aqueous core. In the latter case the protein and TEMPOL were prepared in a molar ratio of 0.85:1.0. Reverse micelles containing the surfactant nitroxide spin label TEMPO-PC (1,2-dipalmitoyl-*sn*-glycero-3-phosphocholine (Avanti Polar Lipids, Inc.) were prepared as above with the additional step of cosolubilizing the TEMPO-PC with the 10MAG and LDAO surfactant mixture in final concentrations of 0.6 mM, 65 mM and 35 mM, respectively. The TEMPO-PC was purchased as 1 mg/mL in $CHCl_3$. An appropriate aliquot was lyophilized in a glass vial and combined with the 10MAG and LDAO aliquot dissolved in hexane. The resulting solution was vortexed and lyophilized again. The dry surfactant mixture was dissolved in 500 μL of deuterated hexane and 0.3 μL of deuterated hexanol. This solution was injected with 18.2 μL of buffer or 6.8 mM ^{15}N flavodoxin C55A, as required, and vortexed until a clear solution formed.

NMR Spectroscopy. ^{15}N HSQC spectra were collected on an AVANCE III 600 MHz Bruker spectrometer equipped with a TCI cryoprobe. Two-dimensional spectral acquisitions included 1024 complex points in the ^1H direct dimension and 200 complex points in the ^{15}N indirect dimension. All spectra were obtained at 25 °C. Data were processed using the AL NMR processing package.[27] The SPARKY graphical analysis software was used to tabulate resonance assignments and associated intensities (Goddard, T.D. and Kneller, D.G. SPARKY 3, University of California, San Francisco).

Paramagnetic relaxation enhancement (PRE) values were determined from the ratio of HSQC intensities of amide $^{15}N-^1H$ correlations in the reverse micelle samples with oxidized (paramagnetic) and reduced (diamagnetic) nitroxide spin label.[23] PRE ratios were normalized to 1.0 using an average scaling factor from the cross peak intensities of the resonances unaffected by the presence of the spin label. Samples were reduced with ascorbate. The ^{15}N and ^1H chemical shift assignments for ^{15}N-labeled flavodoxin (C55A, S72C) were mapped from the aqueous flavodoxin assignments.[22] Mapped assignments were confirmed by tracing the through space connectivities in a 3D NOESY HSQC spectrum collected with a 100 ms mixing time. Samples employing TEMPOL in the water core or TEMPO-PC in the surfactant shell of the reverse micelle were made with ^{15}N-flavodoxin (C55A). The reverse micelle samples with the spin label covalently attached to the protein were prepared with ^{15}N-MTSL-^{15}N-flavodoxin (C55A, S72C).

The ^{15}N NOESY HSQC experiments were collected with 1024 complex points in the acquisition dimension, 64 complex points in the ^{15}N evolution dimension, and 200 complex points in the ^1H indirect dimension. The NOESY mixing time was 100 ms. The water flip back pulse was not used in these spectra to maintain the coherence of the water proton magnetization with the protein proton magnetization. The processed 3D spectra were analyzed at the ^1H water plane to measure the relative intensity of the amide NOE cross peaks to water relative to the amide diagonal cross peaks.

Estimates of the effective macromolecular tumbling time of the encapsulated protein were obtained from the ^{15}N-TRACT measurements using 40 gradient time increments to describe the decay of the relevant α and β ^{15}N transitions[28] essentially as described elsewhere.[29] Exponential decay rates of selected regions of the integrated amide frequencies were fitted using in-house python scripts with Al NMR processing.[27]

EPR Spectroscopy. CW EPR spectra were acquired on an X-band (9.372 GHz) Bruker EMX spectrometer. A modulation amplitude of 1 G was employed, and a 100 kHz modulation frequency using 1 mW of power. Power saturation EPR curves were collected to the maximum available power (300 mW). All reverse micelle solutions tolerated this power. In contrast, aqueous solutions were susceptible to boiling at power levels above 100 mW. Four (4) mm EPR tubes were used for data collection of reverse micelle solutions at room temperature. The EPR spectra of aqueous solutions were collected in Wiretrol 50 μL capillary tubes (0.08 mm i.d.) (Drummond Scientific Co.). Simulations of spectra were carried out with EasySpin.[30]

Dynamic Nuclear Polarization. DNP experiments employed a Bruker ElexSys E580 X-band EPR spectrometer, which was extended with an iSpin-NMR System (SpinCore Technologies, Inc.). For observation of ^1H signals a Bruker MD4-W1 ENDOR probe was used. The RF coil is connected to a tuned RF circuit. Proton NMR spectra

dx.doi.org/10.1021/ja4107176 | J. Am. Chem. Soc. 2014, 136, 2800−2807

were acquired at the magnetic field of the lowest hyperfine line in the EPR spectra of the reverse micelles samples. This corresponded to a carrier frequency of 14.7 MHz. The FID was collected after a single 90 degree pulse of 10 μs. CYCLOPS phase cycling was used. Spectral acquisitions included 128 scans with a 10 kHz sweep width and 512 complex points, and an interscan delay of 4 s. To induce DNP, microwaves were generated at the appropriate frequency with the Bruker X-band bridge. The microwaves were then amplified to 10 W using a Bruker AmpX10 amplifier and directed into the cavity, which was still tuned for continuous-wave EPR. The NMR spectra were processed with an exponential multiplication of 10 Hz, zero filled once and Fourier transformed.

For DNP in solution, the dynamics of the polarizing agent-water interaction largely governs the strength of the polarization transfer via the Overhauser effect. Briefly, the enhancement is usually expressed as:[13]

$$\varepsilon = -\zeta f s \left| \frac{\gamma_s}{\gamma_I} \right| \tag{1}$$

where s is a saturation factor that describes the efficiency of saturation of the electron Zeeman transitions, f is a leakage factor that describes the paramagnetic enhancement of the nuclear relaxation rate over the total nuclear relaxation rate, and ζ is the coupling factor, which defines the magnetization transfer from the electron to the nuclear spin when the electron spin is saturated.

The ^{1}H NMR spectrum obtained at 15 MHz is not resolved. DNP enhancement of the water (ε_{H_2O}) and other hydrogen resonances (ε_{Hother}) were determined by measuring the total integrated intensity of the unresolved ^{1}H resonance obtained with (I_{ON}) and without (I_{OFF}) saturation of the EPR resonance line using samples prepared with H_2O and D_2O using eq 2. The relative contributions of the water (f_{H2O}) and other (f_{Hother}) ^{1}H spins to the spectrum were determined by integration of the high-resolution spectrum obtained at 600 MHz.

$$I_{ON} = f_{H_2O}(\varepsilon_{H_2O} + 1)I_{OFF} + f_{Hother}(\varepsilon_{Hother} + 1)I_{OFF} \tag{2}$$

RESULTS AND DISCUSSION

Introduction of Polarizing Agents into Reverse Micelles. To examine the potential for reverse micelle samples to provide a path to signal enhancement, three types of placement of nitroxide spin radical in the reverse micelle macromolecular assembly were examined: (A) attachment to the protein via a cysteine bridge (MTSL); (B) free in the aqueous core in soluble form (TEMPOL); and (C) embedded in the reverse micelle shell using a carrier lipid (TEMPO-PC) (Figure 1).

Here we use mutants of flavodoxin from cyanobacteria *Anabaena* PCC7119 as a test protein. Flavodoxins function as soluble electron carriers between redox proteins and contain a noncovalently bound flavin mononucleotide cofactor (FMN) that serves as a redox center.[31]

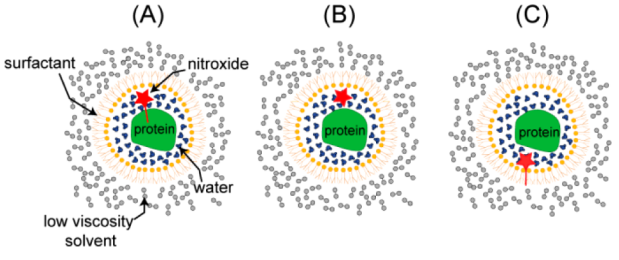

Figure 1. Schematic illustrations of the strategies for introduction of nitroxide spin radicals to reverse micelles. (A) Nitroxide covalently attached to the protein (MTSL). (B) Nitroxide dissolved in the aqueous core (TEMPOL). (C) Nitroxide attached to a carrier embedded in the surfactant shell (TEMPO-PC).

Flavodoxins are characterized by an α/β doubly wound topology, which consists of a five-stranded parallel β-sheet surrounded by α-helices on both sides. The cyanobacteria *Anabaena* PCC7119 protein consists of 179 amino acid residues. The FMN cofactor is noncovalently but tightly bound flavin mononucleotide and was studied here in its oxidized (diamagnetic) state. The structure and dynamics of this flavodoxin have been studied extensively by both crystallography[32,33] and by NMR spectroscopy.[22,34] This protein has also served as a model protein for the development and demonstration of reverse micelle encapsulation.[25,29,35] The C55A mutant from cyanobacteria *Anabaena* PCC7119 is used as a parent molecule in order to avoid slow dimerization through an intermolecular disulfide. For direct ligation of the nitroxide radical to the protein, flavodoxin (C55A, S72C) was created to provide a readily accessible surface cysteine through which a nitroxide spin radical (MTSL) could be attached using standard chemistry.

To form the protein containing reverse micelles, we employ a recently developed surfactant system based on the zwitterionic surfactant lauryl-dimethylamine-*N*-oxide (LDAO) and the nonioinic surfactant 1-decanoyl-rac-glycerol (10MAG).[25] Conditions were chosen to have roughly one nitroxide radical per protein-containing reverse micelle to avoid Heisenberg exchange interactions between nitroxide spin radicals. The protein and corresponding spin label were encapsulated within 10MAG/LDAO reverse micelles in hexane with a water loading of 20. Detailed consideration of the ^{15}N-HSQC spectra of encapsulated flavodoxin in the three scenarios for delivery of the nitroxide radical to the reverse micelle indicates that the structural integrity of the protein is fully maintained (Figure 2).

The general strategy[13] that is being followed for the implementation of dynamic nuclear polarization in aqueous solution is to utilize the rapidly fluctuating interaction of solvent water and spin radical to mediate polarization transfer through the OE. The second and equally important polarization transfer between water and the macromolecule of interest will also proceed via a dipole−dipole interaction albeit with somewhat different physical parameters.[36] Clearly, since sensitivity enhancement is the central goal, it is vitally important that sample size not be overly compromised. Unfortunately, the high dielectric loss of standard aqueous samples requires significant reduction in both sample volume and depth.[13] In contrast, solutions of reverse micelles in liquid alkane solvents are relatively transparent to microwaves.[17−19,37] Though the water core of reverse micelles can have significant dielectric absorption in this frequency region, the overall bulk macroscopic microwave receptivity of reverse micelle solutions is much more favorable than aqueous solutions. This is confirmed here where reverse micelle solutions do not limit the sample diameter or total sample volume. X-band EPR spectra of the three nitroxide labeling scenarios are shown in Figure 3. In contrast, aqueous sample volumes and diameters must be kept an order of magnitude smaller for even simple EPR spectra to be obtained. EPR CW power saturation curves were measured for aqueous MTSL labeled flavodoxin (C55A, S72C) in a 50 μL capillary and MTSL labeled flavodoxin (C55A, S72C) in LDAO/10MAG reverse micelles in a 4 mm tube. The power required for half-saturation for the aqueous solution was 56 mW and 4 mW for the reverse micelle solution, clearly demonstrating the greater microwave receptivity of the

dx.doi.org/10.1021/ja4107176 | J. Am. Chem. Soc. 2014, 136, 2800−2807

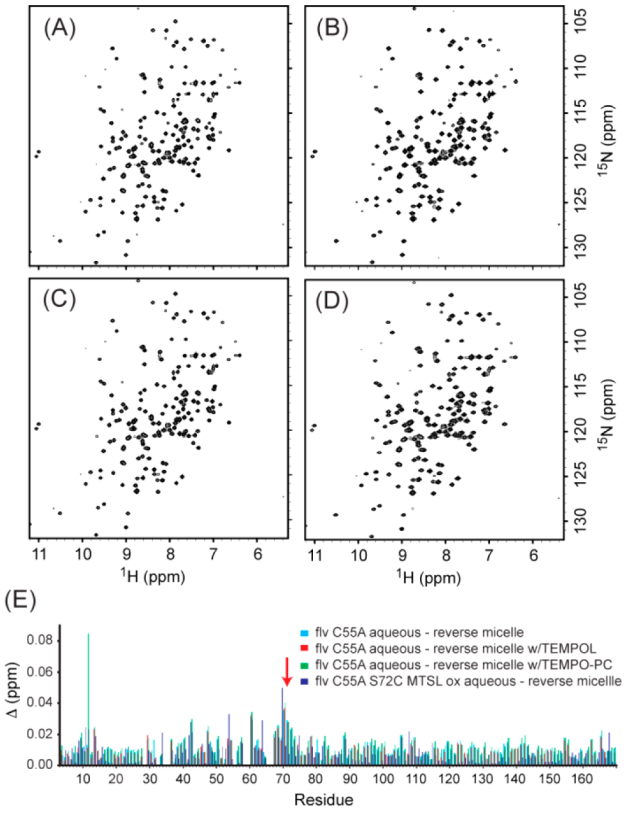

Figure 2. Structural integrity of encapsulated, spin-labeled flavodoxin is maintained. ^{15}N HSQC spectra of (A) ^{15}N flavodoxin (C55A), (B) ^{15}N flavodoxin (C55A, S72C) with ^{15}N MTSL covalently attached, (C) ^{15}N flavodoxin C55A with TEMPOL, and (D) ^{15}N flavodoxin (C55A) with TEMPO-PC. (E) The chemical shift differences ($\Delta = ((\Delta\delta_N\gamma_N/\gamma_H)^2 + (\Delta\delta_H)^2)^{1/2}$) of backbone amide ^{1}H−^{15}N resonances of flavodoxin in free aqueous solution and flavodoxin in 10MAG/LDAO reverse micelles. All residues that could be measured are shown including the site of mutation and ligand attachment (red arrow). Very minor chemical shift perturbations are found (R^2 = 0.999 and <rmsd> = 0.010), indicating that high structural fidelity is maintained upon encapsulation of the protein with spin label in the three labeling scenarios examined (see Figure 1).

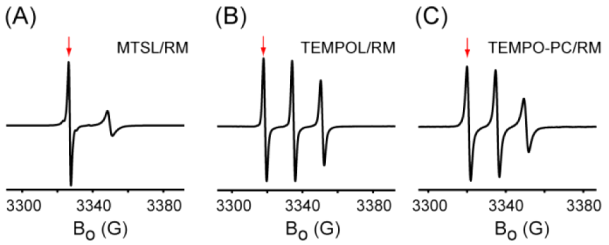

Figure 3. X-band EPR spectra of the nitroxide spin radical in the three labeling scenarios in 10MAG/LDAO reverse micelles. (A) ^{15}N-flavodoxin in the aqueous core and covalently attached to ^{15}N-MTSL (B) ^{14}N-TEMPOL solubilized in the aqueous core with ^{15}N-flavodoxin. (C) ^{15}N-flavodoxin and ^{14}N-TEMPO-PC solubilized in the reverse micelle surfactant shell. The triplet splitting is a result of the spin 1 ^{14}N-electron hyperfine coupling for ^{14}N-TEMPO-PC and ^{14}N-TEMPOL while the doublet splitting arises from the spin 1/2 ^{15}N-electron hyperfine coupling of the ^{15}N-MTSL. These spectra were obtained at 25 °C with 4 mm sample tubes. The red arrow indicates the frequency for the application of the microwave power for the DNP experiments.

latter. The current strategy in the context of solution OE DNP is to employ optimized coil designs with very small sample sizes on the order of μL to nL.[13] This creates at the outset a deficit in signal-to-noise that must be overcome in order for DNP to ultimately prove worthwhile. In this respect, solutions of encapsulated proteins dissolved in low viscosity fluids such as the short chain alkanes largely avoid this issue.

The EPR spectra indicate that the nitroxide moiety experiences variable dynamics depending on context. A rotational correlation time that is slow or comparable to the applied microwave frequency influences the shape of the observed EPR spectrum. To determine rotational correlation times the spectra shown in Figure 3 were simulated with EasySpin.[30] The motion of the MTSL ($\tau \approx 1.5$ ns) attached to the encapsulated protein is slowed relative to TEMPO-PC embedded in the surfactant shell ($\tau \approx 0.15$ ns) and TEMPOL free in the aqueous core of the reverse micelle ($\tau \approx 0.1$ ns). This compares to the motion of TEMPOL in free aqueous solution ($\tau \approx 20$ ps).[38] The effective rotational correlation time of encapsulated flavodoxin, was estimated using the ^{15}N TRACT experiment[28] to be ~12 ns, which is considerably slower than the motion of nitroxide in any of the three labeling scenarios. This has important implications for subsequent optimization of the primary DNP to the water core as discussed below.

Paramagnetic Relaxation Effects. Further analysis also shows the expected presence of paramagnetic relaxation enhancement (PRE) effects (Figure 4). PREs can potentially

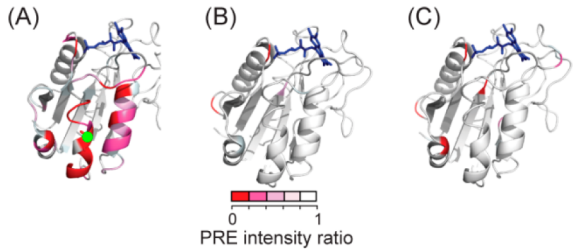

Figure 4. Dependence of paramagnetic relaxation enhancements of the encapsulated protein on the method of nitroxide incorporation. Color-coded PREs of amide ^{15}N−^{1}H correlations of flavodoxin encapsulated in 10MAG/LDAO reverse micelles are mapped onto the 1FLV PDB structure.[33] The FMN moiety is shown in blue. (A) PREs from the MTSL spin label covalently attached at Cys72 (green dot) of encapsulated flavodoxin (C55A, S72C). (B) PREs with TEMPOL in the aqueous core of the reverse micelle with flavodoxin (C55A) encapsulated. (C) PREs with TEMPO-PC solubilized in the surfactant shell of the reverse micelle with flavodoxin (C55A) encapsulated. Structural renderings were generated using PyMol.[39]

counter the desired DNP signal enhancement through introduction of line broadening and other relaxation effects. Used extensively in the characterization of both static and dynamical features of macromolecular structure,[40−43] the deleterious effects of the PRE here arise primarily from long-range coupling of the electron spin with ^{1}H spins. In this regard, the placement of the nitroxide radical within the reverse micelle assembly is apparently important. As expected, the MTSL spin label covalently attached to C72 of flavodoxin (C55A, S72C) gave significant PREs in accordance with expected distant dependence in the region encompassing ~15 Å distances to the spin label (Figure 4A). A number of amide ^{15}N−^{1}H correlations have greatly diminished intensity. This

dx.doi.org/10.1021/ja4107176 | J. Am. Chem. Soc. 2014, 136, 2800−2807

initial result recommends against employing a covalently attached spin radical in the context of DNP utilizing reverse micelle encapsulation. In contrast, nitroxide radical solubilized within the aqueous core or restricted to the surfactant shell show minimal PRE effects (Figure 4B and C).

DNP of the Reverse Micelle Water Core. Dynamic nuclear polarization was obtained by irradiation of the downfield hyperfine transition (see Figure 3). Saturation of the central transition yielded similar results. Microwave power at 9.4 GHz was applied continuously at 10 W during the entire acquisition and the 4 s recycle delay. All reverse micelle solutions tolerated the maximum power employed without significant sample heating. The signal phase was negative for the spectra with the "microwave on" compared to the "microwave off" spectra, confirming that the DNP enhancement is governed by the dipolar-mediated Overhauser mechanism. The resulting ^{1}H spectra are shown in Figure 5.

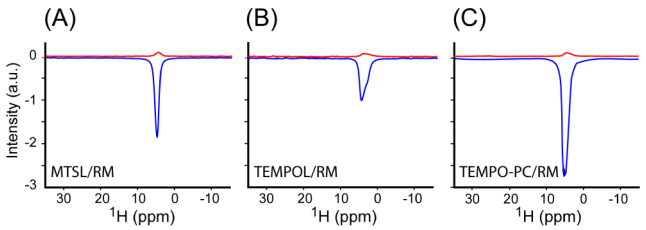

Figure 5. Dynamic nuclear polarization in reverse micelles. ^{1}H NMR spectra (14.7 MHz) of the water core of 10MAG/LDAO reverse micelles with (blue) and without (red) saturation of the 9.4 GHz EPR transition indicated in Figure 3 for (A) ^{15}N-flavodoxin covalently attached to ^{15}N-MTSL and dissolved in the aqueous core; (B) ^{14}N-TEMPOL solubilized in the aqueous core with ^{15}N-flavodoxin; and (C) ^{15}N-flavodoxin in the aqueous core and ^{14}N-TEMPO-PC solubilized in the reverse micelle surfactant shell. Samples were prepared with a W_0 of 20.

To account for variations in line shape, DNP enhancements were calculated using magnetization intensities obtained by integration rather than the maximum of the ^{1}H resonance. The ^{1}H NMR spectrum obtained at 14.7 MHz is not resolved (Figure 6).

In order to isolate the DNP enhancement of the water core from the DNP enhancement of all other contributions to the unresolved ^{1}H spectrum, reverse micelle samples of TEMPOL prepared in D_2O and H_2O were compared. The fractional contributions were obtained by integration of the resolved ^{1}H spectrum obtained at 600 MHz (Figure 6) and the desired enhancements obtained by simple algebra (eq 2).

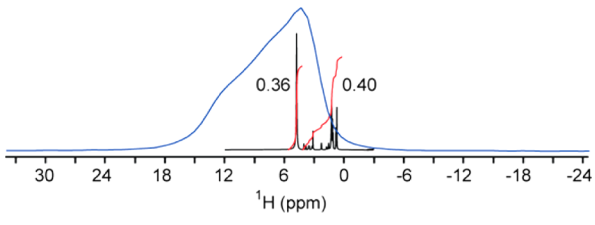

Figure 6. ^{1}H spectra of the reverse micelle solution. Overlay of the 14.7 MHz DNP enhanced ^{1}H spectrum (blue, phase inverted for clarity) onto the 600 MHz ^{1}H spectrum (black) of 400 μM flavodoxin (C55A), 200 μM TEMPOL solubilized in 100 mM LDAO/10MAG reverse micelles at a W_0 of 20. A 10 Hz exponential apodization function was applied to both FIDs. Integration values for the 600 MHz spectrum are indicated for the water resonance and the region containing the resonances due to surfactants and alkane solvent.

In this case, free TEMPOL in the aqueous core of the reverse micelle gave DNP enhancements of the water core (ε_{H_2O}) of -25 ± 9 without protein encapsulated and -34 ± 9 with protein encapsulated. The DNP enhancement for nonwater ^{1}H spins (i.e., those arising from the surfactants and alkane solvent) was small ($\varepsilon_{Hother} \approx -2$) indicating that its hydration shell will undoubtedly dominate polarization of the protein. The value for ε_{Hother} was subsequently used to obtain the DNP enhancements for the water core in all samples. For comparison, free TEMPOL in bulk aqueous solution gave a ε_{H_2O} of ~ -36.

MTSL attached to flavodoxin gave an ε_{H_2O} of -34 ± 9 and TEMPO-PC anchored in the reverse micelle surfactant shell the largest enhancements of the water core ($\varepsilon_{H_2O} = -70 \pm 18$ without protein encapsulated and -93 ± 23 with protein encapsulated). The dependence of the DNP enhancement on water loading (W_o) in the reverse micelle assembly was also evaluated using 400 μM TEMPOL in the absence of protein. Preliminary experiments indicate that the absolute enhancement increases with increasing water loading. The enhancement factors are (within error) insensitive to the presence or absence of encapsulated protein in the reverse micelle, indicating the details of interaction between polarizer and water molecules relevant to DNP are not greatly perturbed by the presence of the protein. It should be noted that the concentrations of water and surfactants is $\sim 10^4$-fold larger than that of the protein, thereby masking DNP of the protein itself.

These initial results suggest that productive DNP enhancements of the water ^{1}H spins can be obtained in the reverse micelle system without compromising sample volume. They also begin to suggest that inclusion of the nitroxide label by association with the reverse micelle surfactant shell or having it free in the aqueous core of the reverse micelle is preferable to anchoring the spin radical to the protein. Other considerations discussed below reinforce this view.

Transfer of Nonequilibrium Polarization from the Water Core to the Encapsulated Protein. A critical component of a possible strategy for dynamically polarizing macromolecules such as proteins is to utilize solvent water as a reservoir of excess polarization.[13] There are at least two potential mechanisms for transfer of nonequilibrium magnetization from water to a protein molecule: hydrogen exchange with solvent and direct dipolar contact between the spins of water and those of the protein. Unfortunately in this context, hydrogen exchange can be significantly slowed within the reverse micelle.[20] On the other hand, the motion of water within the reverse micelle is also significantly slowed, relative to bulk aqueous solution,[44−49] which leads to longer residence times of hydration water at the surface of the protein and more effective dipolar contact with the protein.[20,21] These two mechanisms lead to excess magnetization residing at spins located at or near the surface of the protein which is then envisaged to flow throughout the protein via the well-known spin diffusion phenomenon.[50] The initial transfer of polarization from water to the protein is therefore critical to the basic approach. The transfer of polarization from water to protein was monitored at 600 MHz (^{1}H) by recording a three-dimensional ^{15}N-resolved NOESY experiment of encapsulated flavodoxin (C55A) using a 100 ms mixing time.

dx.doi.org/10.1021/ja4107176 | J. Am. Chem. Soc. 2014, 136, 2800−2807

At pH 8, both the free and encapsulated proteins show a large number of cross peaks with the water resonance, which arise from a combination of direct and relayed NOEs (Figure 7). At pH 5, the hydrogen exchange-mediated transfer is

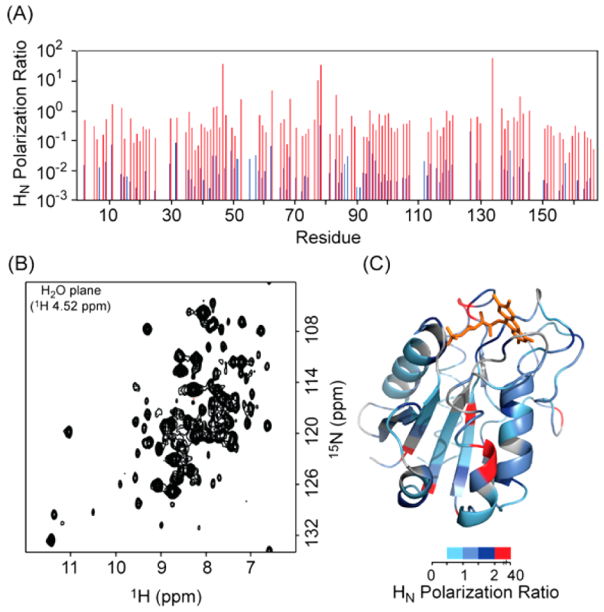

Figure 7. Efficiency of transfer of magnetization between encapsulated protein and the water core at 14 T. (A) Semilog plot of the ratio of the intensity the water NOE cross peak relative to the amide diagonal resonance of a 3D ^{15}N NOESY HSQC for flavodoxin (C55A) encapsulated in LDAO/10 MAG reverse micelles at pH 8.0 in red and aqueous flavodoxin (C55A) at pH 8.0 in blue The NOE mixing time was 100 ms for both spectra. Approximately 90% of the amide hydrogens of encapsulated flavodoxin show NOEs to water. Fewer sites show NOEs to water in the aqueous condition with the intensity ratio reduced by 1−2 orders of magnitude compared to the reverse micelle spectrum. (B) The ^{1}H water plane of the 3D ^{15}N NOESY HSQC spectrum of flavodoxin (C55A) encapsulated in LDAO/10 MAG reverse micelles at pH 8.0. (C) Mapping of the NOE intensity ratio of the water cross peak to the amide diagonal peak onto the three-dimensional structure of flavodoxin (PDB code FLV1).[33] The color bar indicates white through dark blue for stronger NOEs with red indicating resonances that display significant hydrogen exchange with water. These amide hydrogens are located at the edges of secondary structure elements and in loops.

reduced, but the NOEs from the RM cavity water to the protein remain largely unaffected (not shown). The amide polarization ratios of flavodoxin (C55A) at pH 8 demonstrated in Figure 7A show 1−2 orders of magnitude-enhanced polarization for the protein in reverse micelles compared to the same protein in aqueous solution. The general suppression of hydrogen exchange within the reverse micelle is apparently amply compensated by more efficient dipolar contact between water and the protein, thereby preserving the feasibility of moving polarization from the water of the reverse micelle core to the protein.

Future Directions. The initial results presented here suggest that the use of reverse micelle encapsulation holds promise for the implementation of DNP in liquids. In particular, solutions of reverse micelles avoid limitations in sample size due to dielectric heating. It should be pointed out that this advantage is anticipated to persist into the THz region. Though the water core of the reverse micelle has a modest absorption peak in the subterahertz region, the overall absorption of reverse micelles solutions is relatively limited for water loadings applicable to high-resolution NMR of encapsulated proteins.[16] Thus, dielectric heating is not anticipated to limit the application of this approach at higher magnetic field strengths. In addition, the relatively slow motion of water in the hydration layer of encapsulated proteins renders polarization transfer to the protein efficient. These observations indicate that use of reverse micelle encapsulation can overcome two of the main barriers facing the use of dynamic nuclear polarization in solution. Nevertheless, several important issues remain to be resolved. Beyond the practical improvement in instrumentation, two fundamental parameters governing the DNP effect need to be explored in the context of the reverse micelle.

The enhancement factor depends upon the coupling factor (ζ), the leakage factor (f) and the saturation factor (s) (eq 1). It has been suggested that in bulk solution the coupling factor is limiting, because the saturation and leakage factors can be usually made close to 1.[51] The saturation factor can certainly be optimized to approach 1 for even the large sample volumes for the reverse micelle system where application of sufficient gigahertz power is not an appreciable limitation. It is thus important to consider the dependence of the coupling factor and the leakage factor in order to further optimize the reverse micelle for maximum enhancement.

The leakage factor has a dependence on the exchange of magnetization of water hydrogens close to the spin label (bound waters) and the hydrogens in the rest of the water core. The leakage factor is expressed as:[52]

$$f = 1 - T_1/T_{10} \tag{3}$$

with T_1 describing the longitudinal relaxation time of the water hydrogens in the presence of the spin label, and T_{10}, the longitudinal relaxation of the water hydrogens in the absence of the spin label. The water loadings typical for high-resolution protein NMR in reverse micelles (W_0 = 10−20) result in an effective concentration of spin radical on the order of 50 to 100 mM, when the concentration of the spin radical is calculated relative to the volume of the water core. This promotes a higher contribution of paramagnetic relaxation to the total relaxation and thereby tends to push the leakage factor to unity. The reverse micelle system offers the ability to optimize the relaxation characteristics through manipulation of the water loading (see below) and the number and location of polarization agent molecules provided.

For nitroxide radicals, which have no contact contribution to the DNP effect, the coupling factor may be expressed as:[51]

$$\zeta = \frac{5J(\omega_s, \tau_c)}{R_{1\mathrm{para}}} \tag{4}$$

with $R_{1\mathrm{para}} = k[7J(\omega_s\tau_c) + 3J(\omega_s\tau_c)]$ and the correlation time for the dipolar interaction (τ_c) is defined as $\tau_c = (\tau_R^{-1} + \tau_s^{-1} + \tau_M^{-1})^{-1}$, where τ_R, τ_s and τ_M are the reorientation time of the nitroxide, the electron relaxation time, and the nuclear lifetime, respectively. Here k and the spectral density, $J(\omega,\tau)$, both depend on the precise details of the motion modulating the interaction. The functional form of $R_{1\mathrm{para}}$ creates a double dispersion for the coupling constant reaching a maximum at low frequency and dropping to zero at high frequency. Thus, the faster motion of water required to maximize the primary DNP effect is counterbalanced by the slower motion of water

dx.doi.org/10.1021/ja4107176 | J. Am. Chem. Soc. 2014, 136, 2800−2807

needed to enhance polarization transfer to the protein.[36] As noted above, the nature of water dynamics within a reverse micelle can be manipulated,[53] and so there is the opportunity to optimize the overall DNP process by fine-tuning the reverse micelle sample. The observed dependence of the DNP enhancement of water on the water loading supports this view as it is well-known that the dynamics of the water in the reverse micelle core are strongly influenced by its size at low water loadings. Thus, the choice of the water loading value may require a compromise between the effective correlation time of the protein and the dynamics of the water most optimal for DNP. Layered on this consideration is the fact that the net enhancement is scaled by the ratio of the magnetic field at which DNP is performed and that of detection. Clarification of this issue will ultimately determine whether both the DNP and the subsequent NMR experiment can be carried out at the same field or if physical sample shuttling between a lower magnetic field, where DNP will occur, and a higher magnetic field, where the high-resolution NMR experiment is performed, will be required.[54]

The conditions used here for the reverse micelle encapsulation with the nitroxide spin label incorporated are a promising beginning for the application of the DNP enhancement to proteins in solution NMR. The enhancement of ∼90 fold at the water resonance can be evaluated in terms of eq 1 as discussed above. The ratio of gyromagnetic ratios of the electron and proton equal to ∼660 is the absolute maximum achievable. There is still a factor of ∼10 to be gained. The saturation factor (S) is ∼1 based on the EPR saturation curves explored by the CW EPR. The leakage factor (f) was estimated at high field to be ∼0.6. Adjusting the water loading, the type and concentration of polarizing agents, and so on can potentially optimize the leakage parameter. Taking the saturation and leakage factors at face value, the coupling factor (η) is suggested to be ∼0.2, which is significantly below that estimated for nitroxide in bulk aqueous solution.[51] The coupling factor potentially has the most room for improvement and depends on the ps dynamics of the polarizer and water molecules (eq 4). From the line shape analysis of the CW EPR spectra (Figure 3), it is evident that the dynamics can be tuned by the placement of the spin radical in the reverse micelle and with the correlation time of the reverse micelle particle. It is also well-known that the dynamics of the water core of reverse micelle are highly dependent upon water loading.[44] In summary, further increases in the efficiency of DNP of the water core can be potentially achieved through further exploration of sample conditions as well as through continuing improvements in instrumentation.

Although encapsulation of proteins and nucleic acids with structural fidelity and high NMR performance within reverse micelles was introduced some time ago,[15,55] it has not seen general acceptance and use. A perceived difficulty in determining suitable encapsulation conditions and the use of nonstandard apparatus[56] are potential barriers to the method's adoption. Recently, we have developed a robust surfactant system that allows for the encapsulation of proteins with a range of sizes (at least up to 80 kDa) and isoelectric points ($4 < pI < 11$).[25] On the basis of the zwitterionic surfactant LDAO and the nonioinic surfactant 10MAG, high structural fidelity and excellent effective macromolecular tumbling times could be achieved. Although solutions of encapsulated proteins dissolved in the low viscosity short-chain alkanes have more favorable dielectric properties than simple aqueous solutions, they are more limited in the concentration of proteins that can be achieved. With some exceptions, effective concentrations of proteins are generally restricted to less than ∼200 μM. Fortunately, in contrast to aqueous samples, the low conductivity of reverse micelle solutions does not degrade the performance of high-Q cryogenic probes.[57] Nevertheless, by taking advantage of the favorable properties of solutions of molecules encapsulated within reverse micelles, one can anticipate that DNP can overcome this modest limitation in concentration and ultimately provide a significant gain in the sensitivity of solution NMR spectroscopy.

■ CONCLUSION

In summary, the results presented here demonstrate that the reverse micelle encapsulation strategy is a useful starting point for the development of procedures for dynamic nuclear polarization of biomolecules in solution NMR.

■ AUTHOR INFORMATION

Corresponding Author

wand@mail.med.upenn.edu

Notes

The authors declare the following competing financial interest(s): A.J.W. declares a competing financial interest as a Member of Daedalus Innovations, LLC, a manufacturer of high-pressure and reverse micelle NMR apparatus.

■ ACKNOWLEDGMENTS

We thank Li Liang for preparation of proteins. This work was supported by NIH Research Grants RO1 GM085120 and R21 GM107829 (AJW) and P41 EB002026 and EB002804 (RGG) and by NSF Research Grant MCB 115803 (A.J.W.). N.V.N., I.D., and G.M. gratefully acknowledge postdoctoral fellowships from the NIH (GM087099), the Swiss National Science Foundation and the Rubicon Fellowship from The Netherlands NWO, respectively.

■ REFERENCES

(1) Overhauser, A. W. *Phys. Rev.* **1953**, *91*, 476−476.
(2) Carver, T. R.; Slichter, C. P. *Phys. Rev.* **1956**, *102*, 975−980.
(3) Hausser, D.; Stehlik, D. *Adv. Magn. Reson.* **1968**, *3*, 79−139.
(4) Müller-Warmuth, W.; Meise-Gresch, K. *Adv. Magn. Reson.* **1963**, *11*, 1−45.
(5) Griffin, R. G.; Prisner, T. F. *Phys. Chem. Chem. Phys.* **2010**, *12*, 5737−5740.
(6) Barnes, A. B.; Markhasin, E.; Daviso, E.; Michaelis, V. K.; Nanni, E. A.; Jawla, S. K.; Mena, E. L.; DeRocher, R.; Thakkar, A.; Woskov, P. P.; Herzfeld, J.; Temkin, R. J.; Griffin, R. G. *J. Magn. Reson.* **2012**, *224*, 1−7.
(7) Hall, D. A.; Maus, D. C.; Gerfen, G. J.; Inati, S. J.; Becerra, L. R.; Dahlquist, F. W.; Griffin, R. G. *Science* **1997**, *276*, 930−932.
(8) Bajaj, V. S.; Mak-Jurkauskas, M. L.; Belenky, M.; Herzfeld, J.; Griffin, R. G. *Proc. Natl. Acad. Sci. U.S.A.* **2009**, *106*, 9244−9249.
(9) Lesage, A.; Lelli, M.; Gajan, D.; Caporini, M. A.; Vitzthum, V.; Mieville, P.; Alauzun, J.; Roussey, A.; Thieuleux, C.; Mehdi, A.; Bodenhausen, G.; Coperet, C.; Emsley, L. *J. Am. Chem. Soc.* **2010**, *132*, 15459−15461.
(10) Hofer, P.; Parigi, G.; Luchinat, C.; Carl, P.; Guthausen, G.; Reese, M.; Carlomagno, T.; Griesinger, C.; Bennati, M. *J. Am. Chem. Soc.* **2008**, *130*, 3254−3255.
(11) Turke, M. T.; Parigi, G.; Luchinat, C.; Bennati, M. *Phys. Chem. Chem. Phys.* **2012**, *14*, 502−510.
(12) Denysenkov, V.; Prandolini, M. J.; Gafurov, M.; Sezer, D.; Endeward, B.; Prisner, T. F. *Phys. Chem. Chem. Phys.* **2010**, *12*, 5786−5790.

(13) Griesinger, C.; Bennati, M.; Vieth, H. M.; Luchinat, C.; Parigi, G.; Hofer, P.; Engelke, F.; Glaser, S. J.; Denysenkov, V.; Prisner, T. F. *Prog. Nucl. Magn. Reson. Spectrosc.* **2012**, *64*, 4−28.
(14) Neugebauer, P.; Krummenacker, J. G.; Denysenkov, V. P.; Parigi, G.; Luchinat, C.; Prisner, T. F. *Phys. Chem. Chem. Phys.* **2013**, *15*, 6049−6056.
(15) Wand, A. J.; Ehrhardt, M. R.; Flynn, P. F. *Proc. Natl. Acad. Sci. U.S.A.* **1998**, *95*, 15299−15302.
(16) Boyd, J. E.; Briskman, A.; Sayes, C. M.; Mittleman, D.; Colvin, V. *J. Phys. Chem. B* **2002**, *106*, 6346−6353.
(17) Mittleman, D. M.; Nuss, M. C.; Colvin, V. L. *Chem. Phys. Lett.* **1997**, *275*, 332−338.
(18) Yang, L. K.; Zhao, K. S. *Langmuir* **2007**, *23*, 8732−8739.
(19) Zhao, K. S.; Jia, Z. J.; Yang, L. K.; Xiao, J. X. *Chem. Res. Chin. Univ.* **2011**, *27*, 1065−1071.
(20) Nucci, N. V.; Pometun, M. S.; Wand, A. J. *Nat. Struct. Mol. Biol.* **2011**, *18*, 245−249.
(21) Nucci, N. V.; Pometun, M. S.; Wand, A. J. *J. Am. Chem. Soc.* **2011**, *133*, 12326−12329.
(22) Liu, W. X.; Flynn, P. F.; Fuentes, E. J.; Kranz, J. K.; McCormick, M.; Wand, A. J. *Biochemistry* **2001**, *40*, 14744−14753.
(23) Battiste, J. L.; Wagner, G. *Biochemistry* **2000**, *39*, 5355−5365.
(24) Liu, Y. Z.; Kahn, R. A.; Prestegard, J. H. *Nat. Struct. Mol. Biol.* **2010**, *17*, 876−882.
(25) Dodevski, I.; Nucci, N. V.; Valentine, K. G.; Sidhu, G. K.; O'Brien, E. S.; Pardi, A.; Wand, A. J. *J. Am. Chem. Soc.* **2014**, submitted.
(26) Marques, B. S.; Nucci, N. V.; Dodevski, I.; Wang, W. C.; Athanasoula, E. A.; Jorge, C.; Wand, A. J. *J. Phys. Chem. B* **2014**, submitted.
(27) Gledhill, J. M.; Wand, A. J. *J. Biomol. NMR* **2012**, *52*, 79−89.
(28) Lee, D.; Hilty, C.; Wider, G.; Wuthrich, K. *J. Magn. Reson.* **2006**, *178*, 72−76.
(29) Nucci, N. V.; Marques, B. S.; Bedard, S.; Dogan, J.; Gledhill, J. M.; Moorman, V. R.; Peterson, R. W.; Valentine, K. G.; Wand, A. L.; Wand, A. J. *J. Biomol. NMR* **2011**, *50*, 421−430.
(30) Stoll, S.; Schweiger, A. *J. Magn. Reson.* **2006**, *178*, 42−55.
(31) Sancho, J. *Cell. Mol. Life Sci.* **2006**, *63*, 855−864.
(32) Mayhew, S. G.; Tollin, G. *Chem. Biochem. Flavoenzymes* **1992**, *3*, 389−426.
(33) Rao, S. T.; Shaffie, F.; Yu, C.; Satyshur, K. A.; Stockman, B. J.; Markley, J. L.; Sundarlingam, M. *Protein Sci.* **1992**, *1*, 1413−1427.
(34) Stockman, B. J.; Krezel, A. M.; Markley, J. L.; Leonhardt, K. G.; Straus, N. A. *Biochemistry* **1990**, *29*, 9600−9609.
(35) Lefebvre, B. G.; Liu, W. X.; Peterson, R. W.; Valentine, K. G.; Wand, A. J. *J. Magn. Reson.* **2005**, *175*, 158−162.
(36) Luchinat, C.; Parigi, G. *Appl. Magn. Reson.* **2008**, *34*, 379−392.
(37) Li, X. W.; Zhao, K. S.; Yang, L. K.; Xiao, J. X. *Acta Phys.−Chim. Sinica* **2009**, *25*, 1409−1414.
(38) Prandolini, M. J.; Denysenkov, V. P.; Gafurov, M.; Endeward, B.; Prisner, T. F. *J. Am. Chem. Soc.* **2009**, *131*, 6090−6092.
(39) Ayuso-Tejedor, S.; Garcia-Fandino, R.; Orozco, M.; Sancho, J.; Bernado, P. *J. Mol. Biol.* **2011**, *406*, 604−619.
(40) Banci, L.; Bertini, I.; Cavallaro, G.; Giachetti, A.; Luchinat, C.; Parigi, G. *J. Biomol. NMR* **2004**, *28*, 249−261.
(41) Iwahara, J.; Schweiters, C. D.; Clore, G. M. *J. Am. Chem. Soc.* **2004**, *126*, 5879−5896.
(42) Simon, B.; Madl, T.; Mackereth, C. D.; Nilges, M.; Sattler, M. *Angew. Chem., Int. Ed.* **2010**, *49*, 1967−1970.
(43) Schweiters, C. D.; Kuszewski, J. J.; Clore, G. M. *Prog. Nucl. Magn. Reson. Spectrosc.* **2006**, *48*, 47−62.
(44) Fayer, M. D.; Levinger, N. E. *Annu. Rev. Anal. Chem.* **2010**, *3*, 89−107.
(45) Fenn, E. E.; Moilanen, D. E.; Levinger, N. E.; Fayer, M. D. *J. Am. Chem. Soc.* **2009**, *131*, 5530−5539.
(46) Moilanen, D. E.; Levinger, N. E.; Spry, D. B.; Fayer, M. D. *J. Am. Chem. Soc.* **2007**, *129*, 14311−14318.
(47) Piletic, I. R.; Moilanen, D. E.; Levinger, N. E.; Fayer, M. D. *J. Am. Chem. Soc.* **2006**, *128*, 10366−10367.
(48) Piletic, I. R.; Moilanen, D. E.; Spry, D. B.; Levinger, N. E.; Fayer, M. D. *J. Phys. Chem. A* **2006**, *110*, 4985−4999.
(49) Tan, H. S.; Piletic, I. R.; Riter, R. E.; Levinger, N. E.; Fayer, M. D. *Phys. Rev. Lett.* **2005**, *94*, 057405.
(50) Macura, S.; Ernst, R. R. *Mol. Phys.* **1980**, *41*, 95−117.
(51) Bennati, M.; Luchinat, C.; Parigi, G.; Turke, M. T. *Phys. Chem. Chem. Phys.* **2010**, *12*, 5902−5910.
(52) Doll, A.; Bordignon, E.; Joseph, B.; Tschaggelar, R.; Jeschke, G. *J. Magn. Reson.* **2012**, *222*, 34−43.
(53) Levinger, N. E.; Swafford, L. A. *Annu. Rev. Phys. Chem.* **2009**, *60*, 385−406.
(54) Krahn, A.; Lottmann, P.; Marquardsen, T.; Tavernier, A.; Turke, M. T.; Reese, M.; Leonov, A.; Bennati, M.; Hoefer, P.; Engelke, F.; Griesinger, C. *Phys. Chem. Chem. Phys.* **2010**, *12*, 5830−5840.
(55) Workman, H.; Flynn, P. F. *J. Am. Chem. Soc.* **2009**, *131*, 3806−3807.
(56) Peterson, R. W.; Wand, A. J. *Rev. Sci. Instrum.* **2005**, *76*, 094101.
(57) Flynn, P. F.; Mattiello, D. L.; Hill, H. D. W.; Wand, A. J. *J. Am. Chem. Soc.* **2000**, *122*, 4823−4824.